Proceedings of the INMM & ESARDA Joint Virtual Annual Meeting
August 23-26 & August 30-September 1, 2021

TRACKING OF INDIVIDUAL TRISO-FUELED PEBBLES THROUGH THE APPLICATION OF X-RAY IMAGING WITH DEEP METRIC LEARNING

Emily H. Kwapis
Nuclear Engineering Program
Herbert Wertheim College of Engineering
University of Florida
Gainesville, Florida, USA 32611

Dr. Kyle C. Hartig
Nuclear Engineering Program
Herbert Wertheim College of Engineering
University of Florida
Gainesville, Florida, USA 32611

ABSTRACT
A methodology combining X-ray imaging and deep learning was developed to identify and track individual TRISO-fueled pebbles at the entry and exit of a PBMR reactor core. This method exploits the current fuel manufacturing process and leverages an intrinsic fingerprint set in the fuel pebble during fabrication. A database of simulated radiographs of unique TRISO-fueled pebbles was developed using MCNP and used to train a deep convolutional neural network using triplet loss to recognize pebble fingerprints. Distance metric learning was implemented to map the pebble radiographs to a lower-dimensional Euclidean space, where distance metrics could then be used to provide a direct measure of similarity between radiographic images. In this initial demonstration of the Pebble Recognition Algorithm, it is shown that the DNN model can successfully classify pebble fingerprints subject to irradiation-induced shrinkages of up to 0.30% with classification accuracies of 98.70%±2.60%.

INTRODUCTION
Pebble bed modular reactors (PBMRs) are fueled by TRISO-fueled pebbles, which are billiard-ball-sized graphite spheres containing up to 18,000 fuel particles that are less than 1 mm in diameter [1-5]. Up to 400,000 TRISO-fueled pebbles may be contained within a reactor core at one time [6-9], and are continuously circulated in and out of the core during its operation. Fuel pebbles are inserted at the top of the reactor core, travel downwards through the core, and exit at the bottom of the reactor. Burnup measurements are then performed on the pebbles to determine if a pebble is viable for another rotation through the core or if the pebble has exceeded the burnup limit and must be removed from circulation [10]. Presently, pebble identities are not tracked because there is no viable method to tag individual TRISO-fueled pebbles without requiring alterations to the current manufacturing process. The mobility of the fuel pebbles and harsh environment of the reactor present challenges in developing a methodology towards identifying individual fuel pebbles. As the pebble transits the core, abrasion and degradation to the pebble surface occurs, eliminating the possibility of affixing or inscribing a tag or serial number to the surface of each pebble. Alternative approaches that have been proposed include embedding tags within the pebble itself, such as neutron activated dopants that are unique to each pebble and are read using gamma spectroscopy [11]. However, it can be challenging to design and implement radiation hard tags and producing individualized dopant concentrations for tens to hundreds of thousands of fuel pebbles is not the most realistic solution. Additionally, all of these methods introduce additional steps and costs to the current manufacturing process.

Identifying individual TRISO-fueled pebbles and maintaining pebble identity is important for reasons concerning nuclear fuel accountability and safety. It is essential to determine if any fuel pebbles are retained in the reactor for unexpectedly long times because this will result in excessive burnup accumulation [12]. Additionally, maintaining pebble identity offers advantages towards validating computational physics models.

In this work, a new solution is proffered and demonstrated towards tagging individual TRISO-fueled pebbles that exploits the current manufacturing process instead of altering it. During pebble fabrication, thousands of fuel particles are mixed into an amorphous carbon phase, which is then pyrolyzed and compacted into hard graphite spheres [13, 14]. This process results in an arbitrary and unique distribution of particles set within a solid matrix, which can be interpreted as a fingerprint for every individual TRISO-fueled pebble. Because TRISO fuel particles are designed to contain fission products and irradiation induced defects within the particle [2, 5, 13, 15], the particles and the fingerprint are essentially fixed and will not shift significantly during irradiation in the reactor core. By imaging the TRISO-fueled pebble and implementing a deep learning algorithm, this fingerprint can be extracted and individual fuel pebbles can be virtually tagged. To automatically identify and tag individual TRISO-fueled pebbles at the entry and exit of a reactor core, a methodology combining X-ray radiation imaging and deep metric learning with triplet loss is developed and named the Pebble Recognition Algorithm.

THE PEBBLE RECOGNITION ALGORITHM

Introduction to Deep Learning

Deep learning refers to the use of neural networks to search for patterns in data in order to complete some task. Neural networks are complex mathematical functions that aim to mimic the biological processes of the brain. These functions contain a large number of coefficients, or parameters, that must be fitted to training data in order to achieve a desired output. For an image classification task, the neural network learns to predict an identity, or class, for an image by performing a combination of transformations on that image. For example, convolutional neural networks (CNNs) use image processing techniques, such as convolutional filters, to extract and compare details between images. Signals generated from the input layer of the network travel through multiple layers (hidden layers) of the model to the output layer. CNNs can also be described as consisting of two separate sets of layers, where the first set consists of convolutional layers and serves to extract features from the input. These image features are extracted through the application of a combination of linear filters (convolutional kernels), pooling layers, and activation functions. The second set of layers are termed fully connected layers, which serve as classifiers using the extracted features and filters equivalent to the size of the image. Connections between all layers of the network are correlated with connection weights that the model learns by determining how much a signal should be amplified or reduced to produce accurate predictions.

It has been repeatedly demonstrated that convolutional neural networks are very successful at classifying images. Classification accuracies as high as 99.40% and 99.84% has been demonstrated on the CIFAR10 dataset and MNIST dataset, respectively [16, 17]. In these examples, the neural network was trained to output a vector of probabilities that the input image belonged to each class. For more challenging problems where a higher discriminative power is required, this backend of the model can be altered to instead provide a compact representation of the input image, otherwise termed an image vector or embedding. To determine the class the input belongs to, the distance (e.g. Euclidean, angular, etc.) between its representation and other

representations is computed. The partner that results in the minimum distance corresponds to the assigned class. This theory is called distance metric learning (DML) and is commonly applied to the image recognition benchmark.

Necessarily, DML requires objective functions that differ from classification-based functions such as the commonly used cross-entropy loss function. Distance metric learning requires objective functions based on distance metrics, where representations of the same class are separated by smaller distances than representations of different classes. Metric learning aims to maximize inter-class separation while minimizing intra-class separation [18, 19]. This is done by projecting the output of the neural network to a lower-dimensional space, or embedding space, where a simple distance metric (e.g. Euclidean, angular cosine) can be applied to compare images. DML has successfully been applied to the widely used datasets CIFAR10, CIFAR100, and MNIST [20, 21], face recognition [22-25], object recognition, hyperspectral and remote sensing scene classification [26, 27], and action recognition [28]. Using face recognition as an example, both DeepFace and FaceNet teach a neural network to output compact and sparse representations of a person's face by relying on the RGB pixels that make up the input [22, 23]. FaceNet does this by training the network with triplet loss to output l^2-normalized Euclidean embeddings, achieving an accuracy of 99.63±0.09% on the Labeled Faces in the Wild (LFW) dataset [23]. Inspired by this impressive work with deep learning and face recognition, this work will demonstrate the design and training of a deep convolutional neural network using DML with triplet loss towards the nuclear fuel recognition of TRISO-fueled pebbles.

Workflow

The Pebble Recognition Algorithm consists of a combination of radiographic images, a deep learning model, and burnup measurements. Before initial entry of a TRISO-fueled pebble into the core, X-ray radiographs along multiple orientations are taken of the fuel pebble. When the pebble exits the core, imaging is performed again and the DNN is invoked to determine the identity of the pebble. In addition, burnup measurements are also performed on the pebble. Because burnup is a strictly increasing value, as a fuel pebble is retained in the reactor core for longer periods of time, this measurement can be used to restrict the number of comparisons performed by the deep learning model. A pebble that has transited the core multiple times will have a higher burnup value than a fresh pebble that has just entered the core, and hence, there is no need to compare these two pebbles. On average, pebbles transit the core 10-15 times before exceeding the burnup limit [7, 8, 29]. After a pebble exceeds the burnup limit, it is removed from circulation and rerouted to spent fuel storage. The radiographs corresponding to this pebble are then removed from the pebble library. A fresh pebble is added to the reactor core and the pebble library, and the cycle repeats.

Network Architecture and Design

The DNN model is made up of six convolutional layers followed by three fully connected layers, totaling 3.98M parameters. Weights are initialized using a Gaussian distribution with a mean of zero and standard deviation of 0.008. Biases are initialized to zero. 3x3 convolutional filters are applied to all convolutional layers. Average pooling is applied to the first three convolutional layers. Further pooling layers were not implemented because particle information was lost and classification accuracies decreased. This also occurred with max pooling. To speed up learning, batch normalization and the rectified linear unit (ReLU) activation function are applied to every layer of the neural network excluding the output layer. At the output layer, a hyperbolic tangent activation function is applied followed by an l^2 normalizer, producing the pebble embedding for

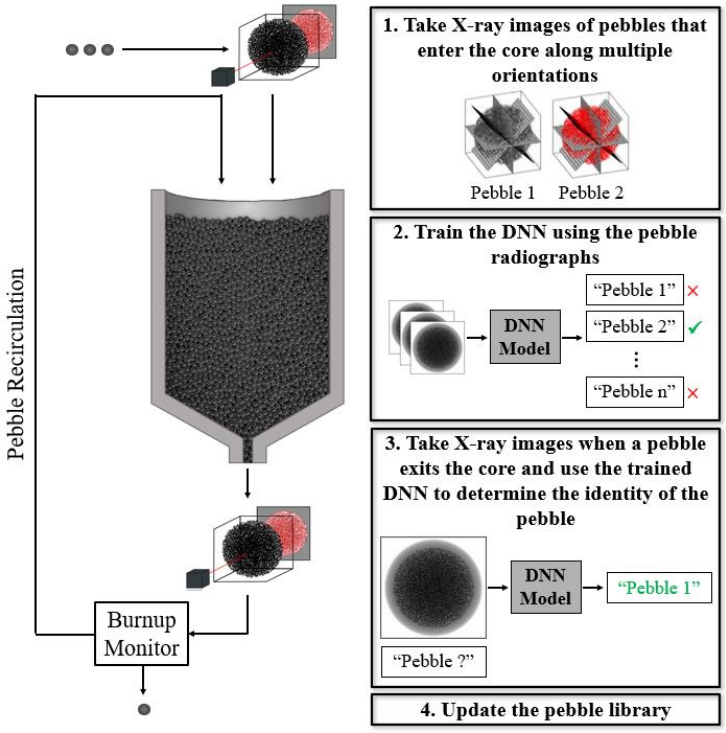

Figure 1. Workflow for the Pebble Recognition Algorithm.

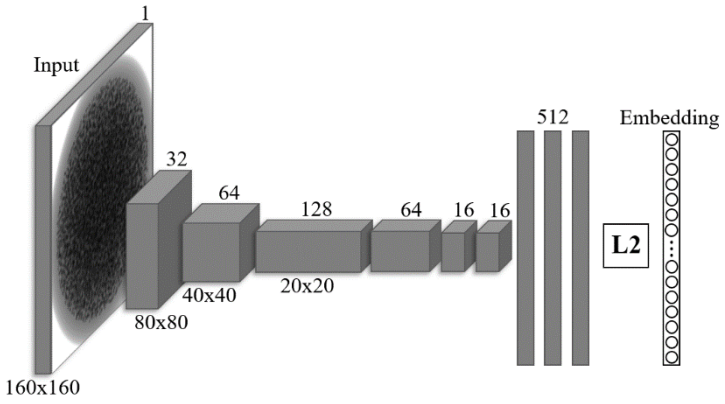

Figure 2. Network architecture of the deep convolutional neural network for the Pebble Recognition Algorithm.

the image. Triplet loss follows the embedding during training and stochastic gradient descent with Nesterov momentum on mini-batches of 64 images is applied. Momentum is set to a value of 0.9 while weight decay is set to 0.0005. The hyperbolic tangent decay scheduler is implemented, with the initial learning rate set to 0.0175. The DNN is trained for 100 epochs.

Objective Function

Triplet loss is implemented with the network architecture for the Pebble Recognition Algorithm. Triplet loss emphasizes inter-class separation and is a common distance metric learning method [23, 27, 30-32]. This objective function minimizes the distance between similar images

(radiographs of the same pebble) and increases the distance between dissimilar images (radiographs of different pebbles). It takes three inputs – an anchor, a positive, and a negative. The anchor is the input image, the positive is an image of the same classification with respect to the anchor, and the negative is an image of a different identity. This work uses Euclidean distance with embeddings in Euclidean space, and the loss function is given by

$$L = \sum_{i=1}^{T} \left[\left\| f(x_i^a) - f(x_i^p) \right\|_2^2 - \| f(x_i^a) - f(x_i^n) \|_2^2 + \alpha \right]_+$$

where x is the input image, $f(x)$ represents the embedding, T is the number of triplet sets, a corresponds to the anchor, p to the positive, and n to the negative, and α is a margin (positive scalar) that must be imposed between the positive and negative pairs.

The selection of triplet pairs plays an important in training the neural network. Hard positives are defined to satisfy the following condition,

$$\text{argmax}_{x^p} \left| |f(x^a) - f(x^p)| \right|_2^2$$

while hard negatives conversely satisfy,

$$\text{argmin}_{x^n} \left| |f(x^a) - f(x^n)| \right|_2^2$$

To speed up convergence, triplets that provide a larger contribution to learning are chosen and are mathematically defined to violate the condition

$$\left| |f(x^a) - f(x^p)| \right|_2^2 + \alpha < \left| |f(x^a) - f(x^n)| \right|_2^2$$

Easy triplets already satisfy this condition, and hence, do not provide a large contribution to learning. Hard positives and hard negatives violate this condition. However, selecting only the hardest triplets during training can have a negative impact on learning and introduce bad local minima and a selection bias. Triplet loss performs better with progressive learning [23, 33, 34]. One method to address these side effects is to use adaptive triplet loss, where the fixed margin is replaced with an adaptive margin $\alpha(a, p, n)$ [21, 35]. Another method is to use semi-hard triplets. Semi-hard triplets violate the condition

$$\left| |f(x^a) - f(x^p)| \right|_2^2 < \left| |f(x^a) - f(x^n)| \right|_2^2$$

and may consist of moderate positives [36] or moderate negatives [23]. In this work, triplets are selectively sampled to predict semi-hard triplets based on moderate positives and hard negatives.

Dataset

A dataset of ~1,250 simulated radiographic images of TRISO-fueled pebbles was produced using Monte Carlo N-Particle (MCNP) Transport code. MCNP has been used in the past for calculations in criticality and neutron flux for pebble bed modular reactors [10, 37]. In these studies, the pebbles were modeled with over 10,000 fuel particles defined within a symmetric lattice filled with graphite. This approach defines identical pebbles, and hence, is not viable for production of a dataset towards use with the pebble recognition algorithm, where every pebble must be unique. To produce a dataset of unique, individual pebbles using MCNP, the location of each fuel particle must be randomized and hardcoded within the graphite pebble sphere. A MATLAB program was written to automate this process and output the MCNP input file. Fuel particle dimensions, fuel type (e.g. UO_2, UCO, Pu), and enrichment vary depending on the manufacturer. The TRISO-fueled pebble MCNP models developed in this work are based on dimensions and material characteristics

taken from A.W. Mehner *et al.* and uses a LEU UO_2 fuel kernel. The Flux Image Radiograph (FIR) tally in MCNP was used to simulate the radiographic images of the TRISO-fueled pebbles. This tally is coupled with the source definition entry, which is defined as a 150 keV X-ray beam, as well as the FM5 flux tally to report the energy deposition of X-rays on an image grid. The image grid is defined as a CsI flat panel detector with a grid spacing of 200 μm. Up to 8 2D radiographs could be generated in an hour on the HiperGator cluster at the University of Florida. A database of CT images was not developed because months of computer time would be required to produce 1,000+ CT images.

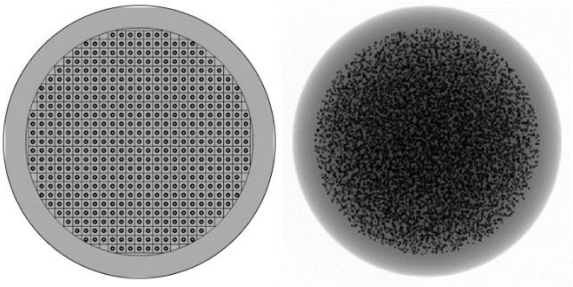

Figure 3. (left) MCNP model of a TRISO-fueled pebble using lattice structures [39] and (right) a MCNP radiographic simulation produced in this work.

The MCNP simulated radiographs consist of 400x400 pixels. To control the number of parameters input into the neural network model, these images are downsampled by a factor of two and centrally cropped, reducing the image dimensions to 160x160 pixels. These pixel values are normalized between 0 and 1, and then standardized by subtracting the mean and dividing by the standard deviation. The dataset is broken into a train set and test set, where 80% of the images are contained within the train set and the remaining belong to the test set.

Data augmentation is performed on all inputs during both training and testing stages of the neural network. Data augmentation is frequently implemented with deep learning algorithms to artificially expand size-limited datasets. The types of data augmentation performed in this work focused on replicating realistic X-ray measurement conditions concerning nuclear fuel. All inputs are randomly cropped by up to three pixels, where a single pixel has an edge size of 565.7 μm, in order to displace the pebbles from being located at the exact center of the image. Padding is then added to the image to maintain the input size. Rotations and flips are also applied to all images. In the extreme environment of the reactor, fuel pebbles will experience irradiation-induced shrinkage. This is simulated by resizing the image, and then, once again applying padding to maintain the original input size of 160x160 pixels. To achieve shrinkage scales less than 1.25% (2/160), a weighted average is taken. On the training set, small dimensional changes are progressively introduced. A simulated irradiation-induced shrinkage of 0.01% is introduced to the training images, and then increased by 0.01% every four epochs until a magnitude of 0.07% is reached. For the test dataset, a random shrinkage magnitude between 0.07% and 0.10% is applied to every image.

RESULTS AND DISCUSSION

The Pebble Recognition Algorithm is trained on a database of simulated MCNP radiographs and achieves a classification accuracy of 93.49%±9.35%, where the error represents differences in performance between multiple runs. An additional preprocessing step of Gaussian smoothing with 3x3 kernels was then applied to the radiographs, and the network was retrained and obtained

improved accuracies and stability at 98.70%±2.60%. Blurring transformations are a common preprocessing technique applied to images before edge detection to smooth out noise associated with uninformative or misclassified edges, which could explain the improved performance with the network model. Additional parameters that can be altered to acquire a higher classification accuracy are the loss function as well as the distance metric associated with the loss function. This work uses triplet loss with Euclidean distance. Recent works with the image recognition algorithms ArcFace and congenerous cosine (CoCo) have reported classification accuracies as high as 99.83% and 99.86% through the use of additive angular margin loss with an arc-cosine distance metric or CoCo loss with a cosine distance metric, respectively [24, 25]. The database of TRISO-fueled pebble radiographs will need to be expanded before investigation into any further alterations to the network model to mitigate overfitting due to repeated training.

Irradiation-induced Shrinkage Limit

The expected magnitude of irradiation-induced shrinkage that TRISO-fueled pebbles will undergo during their tenure in the reactor core is based matrix irradiation performance tests historically performed on fuel pebbles. For irradiation conditions of interest ($< 1400°C, < 9 \cdot 10^{25}$ n/m^2), shrinkage of less than 2% is expected with respect to diameter [13]. On average, pebbles transit the core 10-15 times during their operational lifetime [7, 8, 29]. Therefore, the ability to recognize the pebble fingerprint with particle shifts of 0.20% is a conservative requirement for the Pebble Recognition Algorithm.

To investigate the algorithm capabilities, shrinkage transformations of magnitudes up to 0.35% were applied to the test data and then the irradiated test data was sent through the trained model. It was observed that there was no change in the classification accuracies for shrinkages up to 0.30%, demonstrating that the algorithm can successfully fulfill the irradiation-induced shrinkage requirement. To determine the shrinkage limit, the shrinkage magnitude was increased further to 0.35% where test accuracies quickly dropped to 52.80%±36.52% and great variability in the results was observed.

Orientational Sensitivity and Work Towards Rotational Invariance

The orientation of the TRISO-fueled pebble during radiation imaging plays an important role in the ability of the DNN model to recognize pebble fingerprints. Currently, six orientations – base orientation (MCNP output), clockwise rotation by 90°, counterclockwise rotation by 90°, horizontal flip, vertical flip, and horizontal flip followed by a vertical flip – for each pebble are saved to the pebble library. The performance results previously stated for the algorithm correspond to exact orientation matches to the pebble library. To investigate the sensitivity of the algorithm to image orientations, small rotations (<5°) away from the saved orientations in the pebble library are applied to the test dataset. A performance cost of 2.84%±4.01% is observed for rotations 0.5° away from the saved orientations. At orientations greater than a 1.25° rotation away from the saved orientations, test accuracies decrease significantly indicating that the current model is very sensitive to the orientation of the radiographic inputs. It is believed that the implementation of CT images is the most promising approach towards addressing the challenge of minimizing orientational sensitivity and achieving rotational invariance. Access to real data is necessary to overcome this challenge.

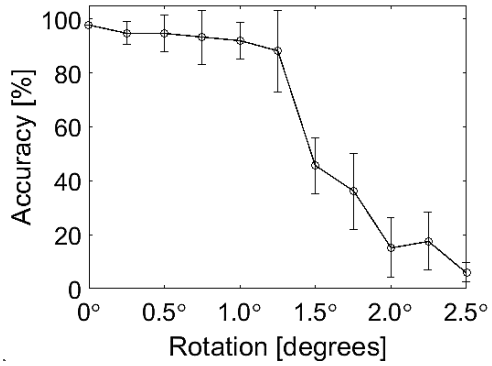

Figure 4. Model sensitivity to small rotations away from saved image orientations in the pebble library.

CONCOLUSION

A methodology combining X-ray radiography and deep metric learning with triplet loss was developed to identify and track individual TRISO-fueled pebbles at the entry and exit of a PBMR core. The Pebble Recognition Algorithm can achieve classification accuracies of 98.70%±2.60% and can successfully classify pebble fingerprints subject to an irradiation-induced shrinkage of up to 0.30%.

ACKNOWLEDGMENTS

This document is the result of research funded partially by the University of Florida Herbert Wertheim College of Engineering, Department of Defense Science, Mathematics, and Research for Transformation (SMART) Scholarship Program, and Department of Energy National Nuclear Security Administration award number DE-NA0003920. The authors would also like to acknowledge their collaborator Dr. Hongcheng Liu in the Department of Industrial and Systems Engineering at the University of Florida who assisted with early attempts to implement algorithms for exploitation of pebble radiographs as well as several fruitful discussions related to machine learning algorithms.

REFERENCES

[1] F.C. de Beer. Neutron- and X-ray radiography/tomography: Non-destructive analytical tools for the characterization of nuclear materials. *J. South Afr. Inst. Min. Metall.*, 115:913-924, 2015.

[2] B. Boer and A.M. Ougouag. Final report on utilization of TRU TRISO fuel as applied to HTR systems part I: Pebble bed reactors. Technical Report INL/EXT-11-21436, FCRD-FUEL-2011-000062, U.S. Department of Energy, Idaho National Laboratory, Idaho Falls, ID, 2011.

[3] M.J. Kania, H. Nabielek, K. Verfondern, and H. Allelein. Testing of HTR UO_2 TRISO fuels in AVR and in material test reactors. *J. Nucl. Mater.*, 441:545-562, 2013.

[4] Nuclear Power Technology Development Section. Fuel performance and fission product behavior in gas cooled reactors. Technical Report IAEA-TECDOC-978, International Atomic Energy Agency, Vienna, Austria, 1997.

[5] P.A. Demkowicz. TRISO fuel: Design, manufacturing, and performance. Technical Report INL/MIS-19-52869-Revision-0. U.S. Department of Energy, Idaho National Laboratory, Idaho Falls, ID, 2019.

[6] A.C. Kadak. A future for nuclear energy: Pebble bed reactors. *Int. J. Critical Infrastructures*, 1(4):330-345, 2005.
[7] A.C. Kadak. MIT pebble bed reactor project. *Nucl. Eng. Tehcnol.*, 39(2):95-102, 2007.
[8] D. Matzner. PBMR project status and the way ahead. In *2nd Int. Topical Mtg. on High Temperature Reactor Technology*, Beijing, China, 2004.
[9] H. Kim, S.H. Kim, and J.K. Kim. A new strategy to simulate a random geometry in a pebble-bed core with the Monte Carlo code MCNP. *Ann. Nucl. Energy*, 38:1877-1883, 2011.
[10] B. Su, A. Hawari, and R. Wood. Design and construction of a prototype advanced on-line fuel burn-up monitoring system for the modular pebble bed reactor. Technical Report DE-FG07-00SF22172 (Project 00-100), 2004.
[11] E.I. Moses, T.D. De La Rubia, J.F. Latkowski, J.C. Farmer, E.K. Storm, and R.P. Abbot. Control of a laser inertial confinement fusion-fission power plant, International Patent WO 2009/058185 A2, May 2009.
[12] H. Chen, L. Fu, G. Jiong, S. Ximing, and W. Lidong. Quantitative analysis of uncertainty from pebble flow in HTR. *Nucl. Eng. Des.*, 295:338-345, 2015.
[13] Office of Nuclear Regulatory Research. TRISO-coated particle fuel phenomenon identification and ranking tables (PIRTs) for fission product transport due to manufacturing, operations, and accidents. Technical Report NUREG/CR-6844, U.S. Regulatory Commission, Washington, DC, 2004.
[14] Electric Power Research Institute. Uranium oxycarbide (UCO) tristructural isotropic (TRISO) coated particle fuel performance: Topical report EPRI-AR-1(NP), Palo Alto, CA, 2019.
[15] Next Generation Nuclear Plant Project. NGNP fuel qualification white paper. Technical Report INL/EXT-10-18610, U.S. Department of Energy, Idaho National Laboratory, Idaho Falls, ID, 2010.
[16] A. Kolesnikov, L. Beyer, X. Zhai, J. Puigcerver, J. Yung, S. Gelly, and N. Houlsby. Big transfer (BiT): General visual representation learning. 2019. arXiv:1912.11370.
[17] A. Byerly, T. Kalganova, and I. Dear. A branching and merging convolutional network with homogeneous filter capsules. 2020. arXiv:2001.09136.
[18] X. Chu, Y. Lin, Y. Wang, X. Wang, H. Yu, X. Gau, and Q. Tong. Distance metric learning with joint representation diversification. In *Proc. Int. Conf. Mach. Learn. (ICML)*, 2020.
[19] A. Taha, Y. Chen, T. Misu, A. Shrivastava, and L. Davis. Boosting standard classification architectures through a ranking regularizer. 2020. arXiv:1901.08616.
[20] B. Zhuang, G. Lin, C. Shen, and I. Reid. Fast training of triplet-based deep binary embedding networks. 2016. arXiv:1603.02844.
[21] B. Yu, T. Liu, M. Gong, C. Ding, and D. Tao. Correcting the triplet selection bias for triplet loss. In *Proc. 15th European Conf.*, Munich, Germany, 2018.
[22] Y. Taigman, M. Yang, M. Ranzato, and L. Wolf. DeepFace: Closing the gap to human-level performance in face verification. In *Proc. 2014 IEEE Comput. Soc. Conf. Comput. Vis. Pattern. Recognit.*, 2014.
[23] F. Schroff, D. Kalenichenko, and J. Philbin. FaceNet: A unified embedding for face recognition and clustering. 2015. arXiv:1503.03832.
[24] J. Deng, J. Guo, N. Xue, and S. Zafeiriou. ArcFace: Additive angular margin loss for deep face recognition. 2019. arXiv:1801.07698.
[25] Y. Liu, H. Li, and X. Wang. Rethinking feature discrimination and polymerization for large-scale recognition. 2017. arXiv:1710.00870.

[26] J. Zhang, C. Lu, J. Wang, X. Yue, S. Lim, Z. Al-Makhadmeh, and A. Tolba. Training convolutional neural networks with multi-size images and triplet loss for remote sensing scene classification. *Sensors*, 20:1188, 2020.
[27] M. Zhang, G. Xu, K. Chen, M. Yan, and X. Sun. Triplet-based semantic relation learning for aerial remote sensing image change detection. *IEEE Geosci. Remote Sens. Lett.*, 16(2):266-270, 2019.
[28] T. Han, H. Yao, W. Xie, X. Sun, S. Zhao, and J. Yu. TVENet: Temporal variance embedding network for fine-grained action representation. *Pattern. Recognit.*, 103, 2020.
[29] F. Vitullo, J. Krepel, J. Kalilainen, H. Prasser, and A. Pautz. Statistical burnup distribution of moving pebbles in HTR-PM reactor. In *Proc. 26th Int. Conference on Nuclear Engineering*, London, England, 2018.
[30] Y. Movshovitz-Attias, A. Toshev, T.K. Leung, S. Ioffe, and S. Singh. No fuss distance metric learning using proxies. 2017. arXiv:1703.07464.
[31] C. Zhang, K. Koishida, and J.H.L. Hansen. Text-independent speaker verification based on triplet convolutional neural network embeddings. *IEEE/ACM Trans. Audio Speech Lang. Process.*, 26(9):1633-1644, 2018.
[32] R. Kumar, E. Weill, F. Aghdasi, and P. Sriram. Vehicle re-identification: An efficient baseline using triplet embedding. In *Proc. Int. Jt. Conf. Neural Netw. (IJCNN)*, Budapest, Hungary, 2019.
[33] G. Hacohen and D. Weinshall. On the power of curriculum learning in training deep networks. In *Proc. 36th Int. Conf. on Mach. Learn.*, Long Beach, California, 2019. arXiv:1904.03626.
[34] T. Castells, P. Weinzaepfel, and J. Revaud. SuperLoss: A generic loss for robust curriculum learning. In *34th Conf. on Neural Inf. Process. Syst. (NeurIPS)*, Vancouver, Canada, 2020.
[35] X. Zhao, H. Qi, R. Luo, and L. Davis. A weakly supervised adaptive triplet loss for deep learning. 2019. arXiv:1909.12939.
[36] H. Shi, Y. Yang, X. Zhu, S. Liao, Z. Lei, W. Zheng, and S.Z. Li. Embedding deep metric for person re-identification: A study against large variations. In *Proc. European Conf. Comput. Vis.*, 2016.
[37] B.M. Makgopa. Simulation of the irradiation behaviour of the PBMR fuel in the SAFARI-1 reactor. Master's thesis. North-West University, 2009.
[38] A.W. Mehner, W. Heit, K. Röllig, H. Ragoss, and H. Müller. Spherical fuel elements for advanced HTR manufacture and qualification by irradiation testing. *J. Nucl. Mater.*, 171:9-18, 1990.
[39] R. Bostelmann, M.L. Williams, C. Cihangir, R.J. Ellis, G. Ilas, and B.T. Rearden. Assessment of SCALE capabilities for high temperature reactor modeling and simulation. In *ANS Winter Meeting and Technology Expo*, United States, 2018.